ISSN 0016-8521, Geotectonics, 2006, Vol. 40, No. 3, pp. 208–224. © Pleiades Publishing, Inc., 2006.
Original Russian Text © O.V. Lunina, A.S. Gladkov, I.S. Novikov, A.R. Agatova, E.M. Vysotsky, A.A. Emanov, 2006, published in Geotektonika, 2006, No. 3, pp. 52–69.

Seismotectonic Deformations and Stress Fields in the Fault Zone of the 2003 Chuya Earthquake, $M_s = 7.5$, Gorny Altai

O. V. Lunina[a], A. S. Gladkov[a], I. S. Novikov[b], A. R. Agatova[b], E. M. Vysotsky[b], and A. A. Emanov[c]

[a]*Institute of the Earth's Crust, Siberian Division, Russian Academy of Sciences, ul. Lermontova 128, Irkutsk, 664033 Russia*

e-mail: lounina@crust.irk.ru

[b]*Institute of Geology, Siberian Division, Russian Academy of Sciences, pr. Akademika Koptyuga 3, Novosibirsk, 630090 Russia*

[c]*Geophysical Survey, Siberian Division, Russian Academy of Sciences, pr. Akademika Koptyuga 3, Novosibirsk, 630090 Russia*

Received July 4, 2005

Abstract—The seismotectonic deformations related to the Chuya earthquake September 27, 2003 in the Gorny Altai ($M_s = 7.5$) are studied in detail. These deformations developed as advanced systems of R- and R'-shears, gash fractures, and compression structural features in loose sediments. In bedrocks, the older shear zones were reactivated, the previously existing fractures were renewed and propagated further, and new faults and crush zones were formed. The system of seismic dislocations is a fault zone no less than 4 km wide that extends in the northwestern direction. As follows from the structural elements that reveal a systematic mutual orientation, the internal structure of this zone is typical of a right-lateral strike-slip fault. The initial stress field that led to the development of the entire assemblage of seismotectonic deformations related to the Chuya earthquake corresponds to the strike-slip type with the NNW, almost meridional direction of compression axis (σ_1) and the ENE, almost latitudinal direction of the tension axis (σ_3). The local variations of the stress state were expressed in an insignificant shift of σ_1 to the northwest or northeast, in the short-term change of relative stress values with retention of their spatial orientation, and in the increasing inclination of σ_1 in front of the previously existing fault. The comparison of the internal structure of the seismotectonic fault zone with a tectonophysical model of faulting in large continental systems with a right-lateral offset indicates that the distribution of the advanced faults corresponds to the late stage of faulting, when the main fault is still not formed completely, but its particular segments are already developed distinctly. It is shown that at high rates of displacement the structural features in markedly different rocks develop according to the general laws of solids' deformation even near the day surface.

DOI: 10.1134/S0016852106030058

INTRODUCTION

The Chuya earthquake with $M_s = 7.5$ happened on September 27, 2003, and was the strongest in the southeastern Gorny Altai over the entire period of instrumental seismological observations (Fig. 1A). In contrast to the Mongolian and Gobi Altai, well known for catastrophic earthquakes [20, 24], only two strong seismic events have been recorded in the Gorny Altai and its nearest framework [12, 24]: September 21, 1923, with M = 6 and June 14, 1990, with M = 6.6–6.9.

The epicentral domain of the former earthquake was not visited by specialists, and its exact location remains unknown. The hypocenter of the main shock of the second earthquake was located at a depth of 35–40 km, and the surface deformations were weak. Only small fractures, fallouts of mud and water-saturated sand from fissures and gryphons, and small landslides were noted [24].

The Chuya earthquake is unique in comparison with the earthquakes mentioned above. First, its epicenter was located in the center of the local network of stations developed by the Geophysical Survey of the Siberian Division, Russian Academy of Sciences, in August 2002, a circumstance that allowed the seismic process in the epicentral domain to be studied before and after the Chuya earthquake [6, 12]. Second, an extended zone of seismotectonic deformations was formed as a result of the earthquake. Third, a considerable segment of this zone is accessible to detailed field examination [2–4, 10].

The results of the field reconnaissance of the epicentral domain of the Chuya earthquake were published first by Geodakov et al. [4]; these researchers traced the NWN-trending system of surface seismotectonic faults for a distance of 20 km. Our investigations carried out in May 2004, have shown that the seismic faults are traceable for more than 30 km [30]. In July 2004, Vysotsky et al. [3] expanded the study area and established that the zone of surface deformations extends for more than 56 km and its width locally reaches a kilometer.

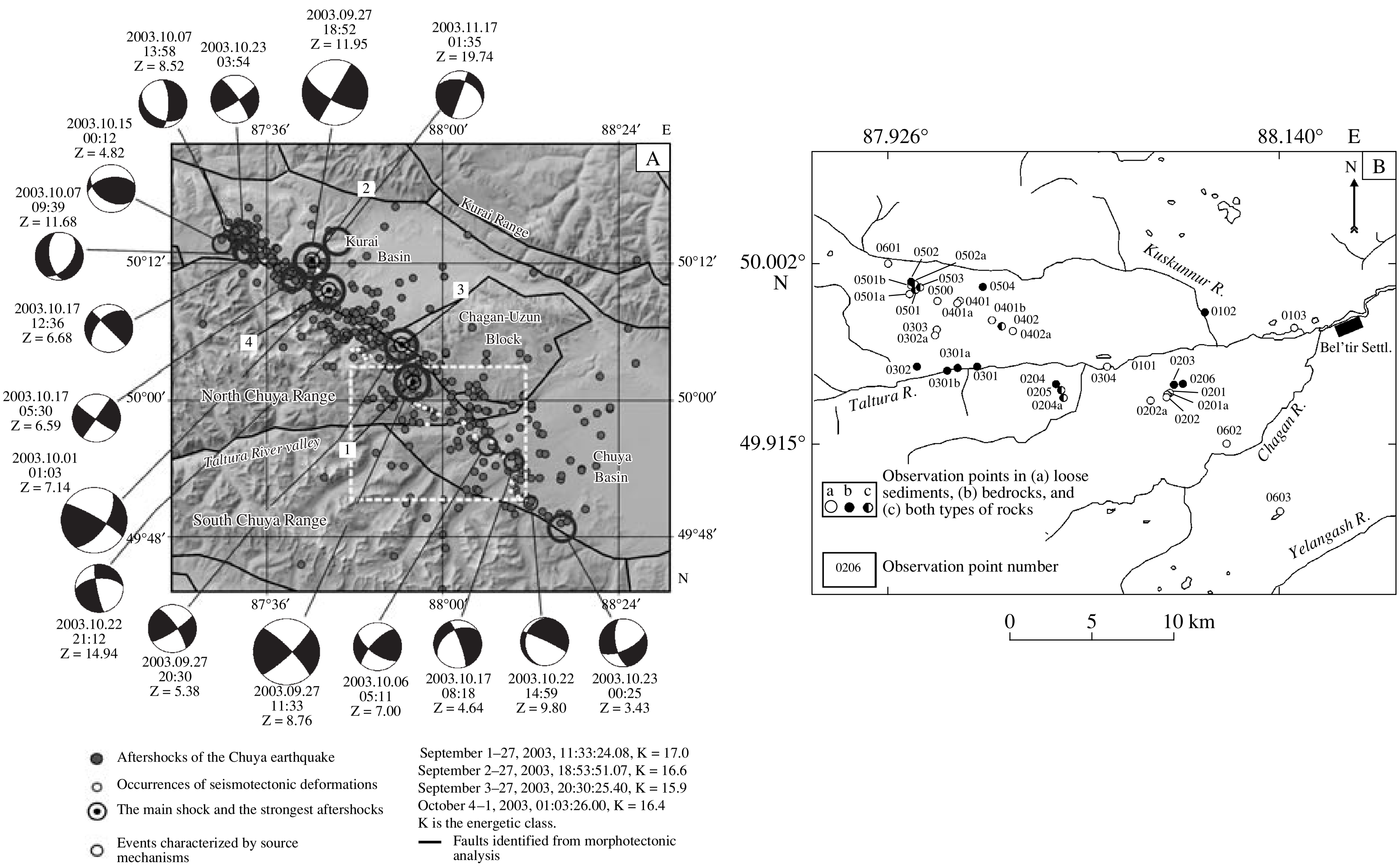

Fig. 1. The epicentral domain of the Chuya earthquake and the area of detailed geological–structural and tectonophysical investigations. (A) The strongest seismic events in September and October 2003, surface seismotectonic deformations traceable for a distance of 56 km, and source mechanisms of the main shocks and aftershocks. The data on epicenter location, source depth (Z), and source mechanisms were obtained by the Geophysical Survey, Siberian Division, Russian Academy of Sciences. The area of detailed investigations shown in panel B is contoured by a dashed line. (B) Location of observation points and their numbers.

In our investigation, the traditional seismogeological observations were supplemented by tectonophysical analysis that allowed us (1) to study the internal structure of the newly formed zone of seismotectonic faults in terms of the laws of deformation of solids, (2) to establish the relationships between the previously existing and newly formed fault systems, and (3) to reconstruct the stress fields associated with seismic events of 2003. The solution of these problems not only contributes to the regional tectonics of the Gorny Altai but also provides insights into the general evolution of seismotectonic deformations and confirms the tectonophysical model of faulting within continental fault zones.

REGIONAL TECTONICS: A BRIEF OVERVIEW

The Gorny Altai within the borders of the Russian Federation is regarded either as the western branch of the Altai–Sayan Fold System and/or as the northern extension of the Mongolian and Gobi Altai [4, 12, 13]. All these mountainous systems are constituents of the Central Asian Mobile Belt. The southeastern Gorny Altai comprises the Kurai, Aigulak, North Chuya, South Chuya, and Chikhachev mountain ranges and the Ukok and Sailyugem plateaus divided by the Sorulukol, Kurai, Chuya, Samakha, Tarkhatty, and Bertek river valleys and intermontane basins. The elevation marks are at a height of 2000 m asl. The floors of depressions subside lower, while the crests of mountain ranges are often higher than 3500 m.

According to the current knowledge, the Earth's crust in the Altai region is broken into numerous blocks and experiences predominant compression in the NNE–SSW, N–S, and NNW–SSE directions [8, 9, 12, 17]. These directions are consistent with the orientation of horizontal displacements established from GPS geodetic data [15]. However, the relatively steady orientation of the axes of maximal shortening is combined with the complicate mosaic seismotectonic deformation field deduced from mechanisms of earthquake sources. As a result, the orientation of the principal axes of deformation and its intensity in particular blocks are variable [9]. The local shearing and extensional deformation are also rather abundant against the background of prevalent compression [17]. Most researchers suggest that the recent tectonic evolution of the region under study was controlled by collision of the Indian and Eurasian plates that gave rise to the offsets along the master strike-slip faults of the Altai [1, 12, 15, 22, 25].

The seismic events in September and October 2003 occurred in the southeastern Altai at the junction of the North and South Chuya ranges with the Kurai–Chuya system of intermontane basins. The main shock in a sequence of earthquakes was localized between the North Chuya and Chagan-Uzun blocks (Fig. 1A) that divide the Kurai–Chuya system into the two depressions underlain by the Paleozoic basement and filled with Cenozoic sediments. The fault pattern of the southeastern Altai was studied largely by seismogeological and geomorphic methods [7, 12, 13, 28]. The main faults extend in the NW direction. The near-latitudinal fault that separates the North Chuya and South Chuya neotectonic blocks is expressed in topography as the Taltura River valley (Fig. 1A). The NE-trending faults are second in importance. In the opinion of most researchers, the deep-rooted latitudinal and northwestern faults are the main features that control seismic events, although the faults of other orientations also bear indications of the Pleistocene and Holocene reactivation. The paleoseismic faults typical of earthquakes with magnitudes reaching 7.5 or even higher were noted in the Kurai–Chuya system of basins and at the adjacent territory [13, 28].

RESEARCH METHODS

A network of points of geological–structural and tectonophysical observations was developed over the area about 30 km in extent from the Yelangash River to the Kuskunnur River in order to study the internal structure of the fault zone and stress fields in the epicentral domain of the Chuya earthquake (Fig. 1B). This is an area of intensely dissected topography at the western closure of the Chuya Basin, where a system of seismotectonic faults is clearly expressed at the surface, while crossing valleys and drainage divides. The valleys and partial divides are covered by middle and upper Pleistocene and Holocene boulders, pebbles, sandy clay, and sand. The bedrocks are mainly represented by the Devonian crystalline schists that crop out at walls of streams and at mountain summits. The field examination at an observation point (OP) included description, photography, and measurements of the spatial parameters (dip and/or strike azimuths and dip angle) and kinematic parameters (slickenside striation, marker offsets) of seismotectonic faults and associated structural features in loose sediments and at rocky outcrops. Special attention was paid to the crush zones, foliation, fracturing, and relationships between the faults that were formed during the Chuya earthquake and had existed previously. The data obtained were used to map and thoroughly distinguish the internal structure of the seismotectonic fault zone and the network of older faults.

The mass measurements of fracturing were performed at 21 of 36 observation points. The results have been represented as diagrams assigned for revealing the conjugated fracture systems with the Nikolaev method [11] and for particular solutions of stress fields. The axes of principal normal stresses were reconstructed on the basis of the following relationships: (i) the line of intersection of two conjugated shear planes coincides with the intermediate stress vector (σ_2), (ii) the axis of principal compressive stress (σ_1) is a bisector of the acute angle between the fractures, and (iii) the axis of principal tensile stress (σ_3) is a bisector of the obtuse angle [5]. In OP 0301, where the slickenside striation determines the displacement unequivocally by the offset of markers, the stress field was reconstructed additionally with the kinematic method [32] substantiated by Angelier [19]. The obtained particular fault-plane solutions characterize local variations of the stress state in the seismotectonic fault zone.

The reconstruction of the general regional stress field, which initiated the Chuya earthquake and gave rise to the formation of the entire structural assemblage of deformations, is based on the results of the complex analysis, which include internal structural features of the seismotectonic fault zone, measured offsets, and spatial patterns of fracturing and slickenside striation.

RESULTS

Seismotectonic Deformations in Loose Sediments

The seismotectonic deformations in loose sediments are sufficiently evident and comprise the following structural features:

(1) systems of advanced shears known as R- and R'-shears (Fig. 2),

(2) gash fractures (Fig. 3A), and

(3) compressive features (Figs. 3B, 3C).

The advanced fractures appear and develop within a fault zone before the appearance of the main fault plane [14, p. 9]. Riedel shears (R- and R'-shears) are the most abundant fractures of this type.

As follows from the distribution of seismotectonic structural elements (Fig. 4A), the NW-trending dislocations (280°–350° NW) are predominant; the distinct maximum (290°–330° NW) corresponds to the R-shears. The R'-shears are not expressed so distinctly and extend along an azimuth of 350° NW–30° NE. The shear fractures are characterized by opening that varies from a few centimeters to a few meters, often as a result of gravitational effects. The horizontal displacements are recorded reliably in offsets of fracture walls (Figs. 5A–5C, 5F). The rose diagrams of shear fractures with various directions of slip show that the NW- and WNW-trending fractures are characterized by right-lateral offsets (Fig. 4B), whereas the NE- and NNE-trending shears are characterized by left-lateral offsets (Fig. 4C). The maximal right-lateral strike-slip offset (2.5 m) was measured at OP 0402 along the fracture striking 290° WNW. The maximal left-lateral offsets (0.2 m) were noted at OPs 0601 and 0603 along the fractures striking 10° and 25° NNE. The vertical displacements are observed less frequently. The greatest normal separations (1 m at OP 0402) are typical of the NW-trending fractures, while the greatest reverse separations are characteristic of the fractures oriented in the ENE direction. The visible depth of continuous fractures reaches tens of meters to a few hundred meters, and downward they are filled with debris. According to eyewitnesses, speleologists descended to a depth of 50 m a year after the earthquake.

The distribution of advanced fractures is characterized by pronounced differentiation. In some cases, we deal with one or two distinct near-parallel fractures and smaller cracks, the density of which is not great in comparison with other sites in the fault zone (Fig. 2B). Such segments are complicated by separate transverse fractures (Fig. 2C). The segments of this kind alternate with areas of highly concentrated, en echelon arranged systems of advanced fractures (Fig. 2E). The structure of the zone looks especially complex at intersections of R- and R'-shears (Fig. 2D), where the offsets along fractures of the same direction may be opposite. A seismic landslide over an area of ~1×0.85 km^2 occurred at a fault intersection on the right slope of the Taltura River valley (Fig. 6). Two older landslides are situated nearby, being located farther away from the tear-off wall, thus indicating that catastrophic earthquakes in the southeastern Altai also happened in the past.

The detailed consideration of the structure of advanced fractures in loose sediments allowed us to establish the dynamics and conditions of their propagation. First, they make up systems of short (<1 m) conjugated fractures of the lower hierarchical level (Fig. 5A). The opposite displacements along these fractures resulted in the formation of rhomb-shaped blocks (Fig. 5B) and pull-apart structural features (Fig. 5C). In turn, these phenomena have determined the general sinusoidal pattern of advancing fractures of various extents and probably mirror propagation of seismic vibrations (variations of direction and amplitude of seismic waves) in the elastic medium. Second, some facts (Figs. 5D–5F) testify that, despite numerous inclusions of hard rocks and tree stumps, the medium reacted to the dynamic impact in the process of faulting as a homogeneous body.

The gash fractures commonly located at tips of R-shears are represented by trenches 2–7 m wide (Fig. 3A). The compressive structural features are expressed largely as swells and hillocks (Fig. 3B) 12–15 m long. Their extent may increase on slopes. Folds were observed at OP 0601 (Fig. 3C). In spite of the seismogravitational origin of the folds, the coinciding generalized orientation of their hinges (80° ENE) and the WNW-trending right-lateral strike-slip fault that is traceable nearby indicate that the folds and fractures were formed in the common field of stress. The gash fractures and compressive features are perpendicular to one another (340°–350° NNW and 70°–90° ENE, respectively), as seen in Figs. 3D and 3E.

The systematic mutual orientation of deformational features in loose sediments shows that the internal structure of the NW-trending deformational zone that was formed during the Chuya earthquake is typical of the right-lateral strike-slip fault.

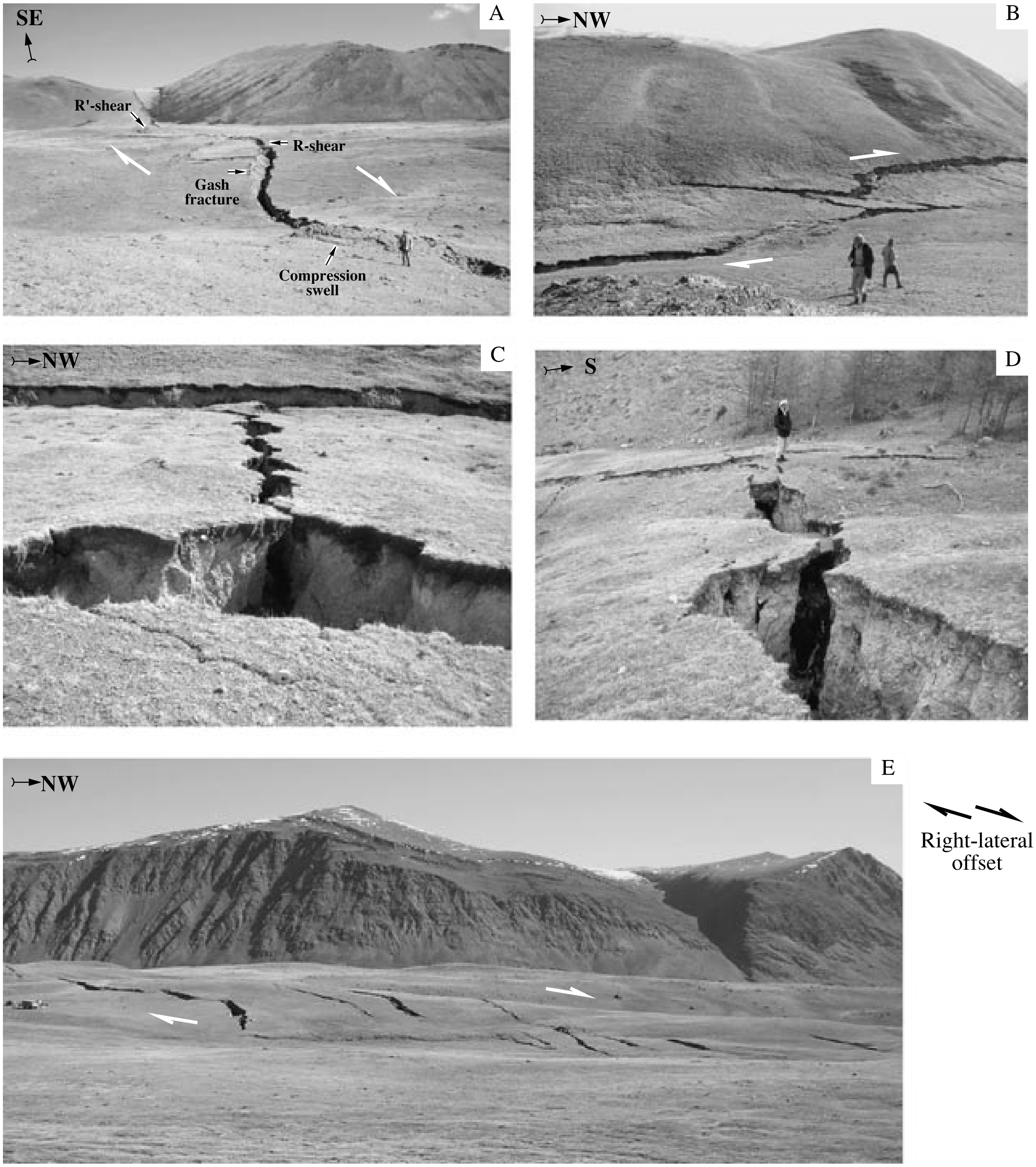

Fig. 2. Seismotectonic strike-slip faults in the Pleistocene and Holocene sediments. (A) General view of the large fault at the drainage divide of the Taltura and Kuskunnur rivers, (B) near-parallel faults at OP 0402, (C) transverse fault that connects two near-parallel dislocations at OP 0402 (close-up of panel B), (D) intersection of faults at OP 0202, and (E) en echelon arranged fracture system at the drainage divide of the Taltura and Kuskunnur rivers.

Seismotectonic Deformations in Bedrocks

The explicit seismotectonic deformations related to the Chuya earthquake were observed in bedrocks at OPs 0203, 0204a, 0205, 0301, 0301a, 0501, 0502a, 0503, and 0504 and are expressed in the following:

(1) reactivation (opening) of older shear zones and rejuvenation of particular fractures with offsets reaching a few decimeters (Figs. 7A, 7B),

(2) growth of previously existing steeply dipping fractures (Fig. 7C), and

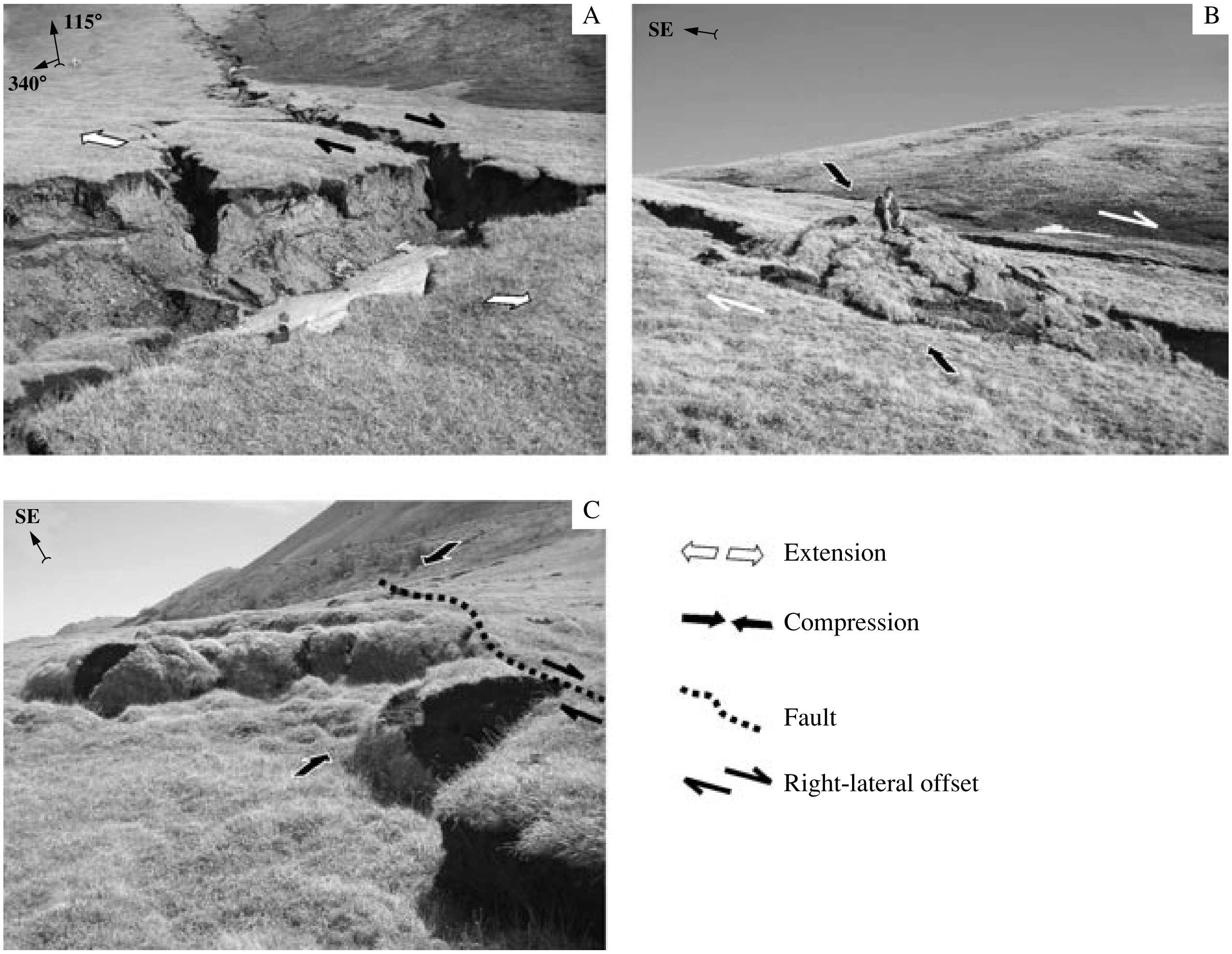

Fig. 3. Seismotectonic deformations in the Pleistocene and Holocene sediments that complicate large strike-slip faults. (A) Gash fracture in combination with an advanced shear fracture at OP 0401b, (B) compression swell between Ops 0401b and 0402, and (C) folds at OP 0601.

(3) formation of new faults and crush zones (Figs. 7D–7F).

The NW-trending and near-latitudinal older thick fault zones are the most favorable for reactivation. The more broken the crystalline massif, the greater the body involved in deformation by means of low-amplitude displacements along short (<2 m) fractures. A striking example of such seismotectonic deformations was observed at OP 0301 in the fault zone no less than 80–100 m thick that extends along the Taltura River (the dip azimuth is 355°–0° N and the dip angle is 80°–85°). In the less disturbed rocky outcrops, the seismotectonic fissures with a gap of 0.1–0.3 m were formed along the sealed shear zones. The continuous fissures are traced through the bedrock and extend into the loose sediments (Fig. 7A). The small rejuvenated and newly formed fractures are arranged en echelon relative to the master faults, thereby indicating the right-lateral offset (Fig. 7B).

The obvious indications of fast propagation of previously existing steeply dipping fractures were observed at OP 0504 (Fig. 7C) on the right bank of the Kuskunnur River. The zones of rough crushing 0.2–3.0 m thick that dip along an azimuth of 20°–30° NNE at an angle of 80°–85° (Fig. 7D) and 110° NE at angles 75°–80° were formed here in slightly fractured, almost monolithic crystalline schists with a "welded" near-horizontal schistosity and sporadic near-vertical fractures.

The distinct seismotectonic faults varying from tens of meters to a few hundred meters have been documented on the northwestern slope and at the top of Mount Nomodokl at OPs 0502a and 0503 (Figs. 7E, 7F). Here, the variously oriented dislocations make up a complex cluster of faults. Both right- and left-lateral offsets are observed along particular segments of the large NW-trending faults. The same situation is also typical of the NE-trending faults. The opposite offsets along the faults of the same direction are probably caused by a different velocity of motions of blocks that

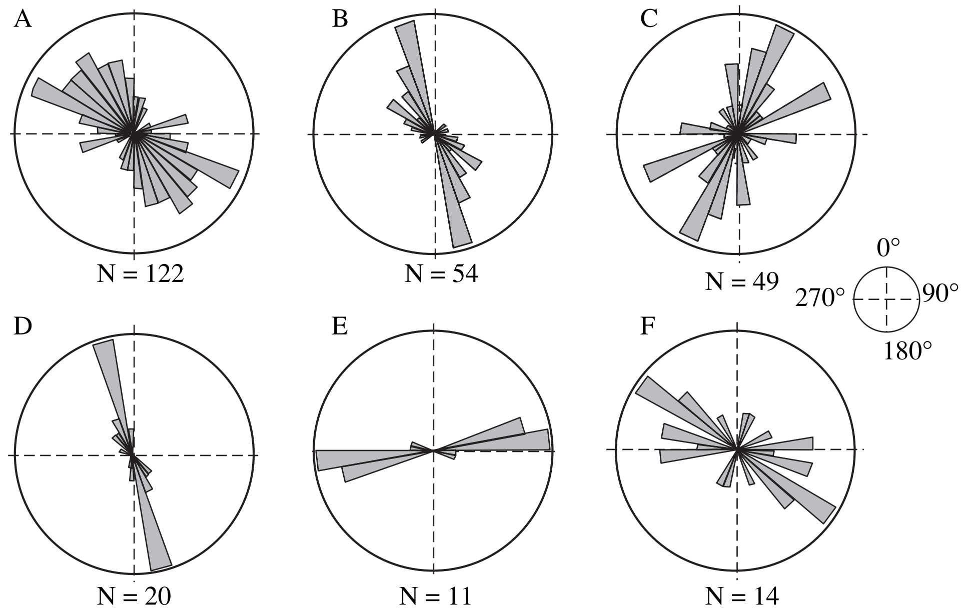

Fig. 4. Rose diagrams of the orientation of various structural elements in the fault zone. (A) Seismotectonic faults in loose sediments, (B) seismotectonic fractures with right-lateral offset, (C) seismotectonic fractures with left-lateral offset, (D) extension fractures, (E) long axes of compression swells, and (F) large seismotectonic faults that dissect bedrock outcrops. N is the number of measurements. Window of averaging is 10°.

were formed in this fault cluster during the Chuya earthquake.

The predominant strike of the documented seismotectonic faults that cut the exposed bedrocks is 300°–320° WNW (Fig. 4F). The rejuvenated faults striking along azimuths of 330°–340° NW, 20°–30° NNE, and 80°–110° E are also noted. On the whole, the orientation, kinematic characteristics, and mutual relations of seismic dislocations observed in bedrocks are similar to those observed in loose sediments.

Relationships between the Previously Existing and Newly Formed Fault Systems

To estimate the degree of inheritance of the older structure by the seismotectonic faults related to the Chuya earthquake, we compiled two schemes of the fault pattern of the study area. The first scheme demonstrates the zones of crushing, schistosity, and fracturing that were documented in the pre-Cenozoic bedrocks. This scheme exhibits the fault network that existed before the Chuya earthquake (Fig. 8A). This pattern is characterized by the NW-trending and near-latitudinal master faults with fault zones more than 5 m thick and the auxiliary NNE-trending faults with fault zones less than 5 m thick. In the central part of the area, the most extended master faults intersect one another, thus making up a large node. As judged from the character of crushing and fracturing, the tectonic lines initially were strike-slip faults; however, their geometric relationship does not allow these faults to be regarded as conjugated dislocations. It is most likely that they developed as independent structural features, and each of them could have generated significant seismic events. This suggestion is supported by the tectonic model proposed by Şengör et al. [30]. According to this model, the strike-slip faults of various directions were of crucial importance during the entire Paleozoic evolution of Asia. In the Gorny Altai, such a tectonic style remained in the Cenozoic. The NW- and NNE-trending faults in the study area could have developed contemporaneously in the Neogene and Quaternary and have retained their activity to date as conjugated strike-slip faults formed under near-meridional compression and near-latitudinal extension.

The second scheme based on the entire data set concerning the studied seismotectonic deformations demonstrates the internal structure of the NW-trending fault zone that formed as a result of the Chuya earthquake (Fig. 8B). This scheme bears information on the kinematics of fractures and the most significant displacements measured during the field work. The most extended systems of advanced R-type fractures and the most significant (by both length and width) fracture zones of the R'-type are designated in the scheme as the main seismotectonic faults. Figure 9B is a summary of all internal structural features described above. Above all, the nonuniform distribution of the advanced fractures should be pointed out. They are expressed as separate large dislocations in some cases and as en echelon arranged systems of small fractures in other cases. In general, the combination of all types of the newly formed structures is a common assemblage that consists of the NW- and NNW-trending right-lateral strike slip faults, occasionally with normal-fault or pull-apart components; the NE- and NNE-trending left-lateral

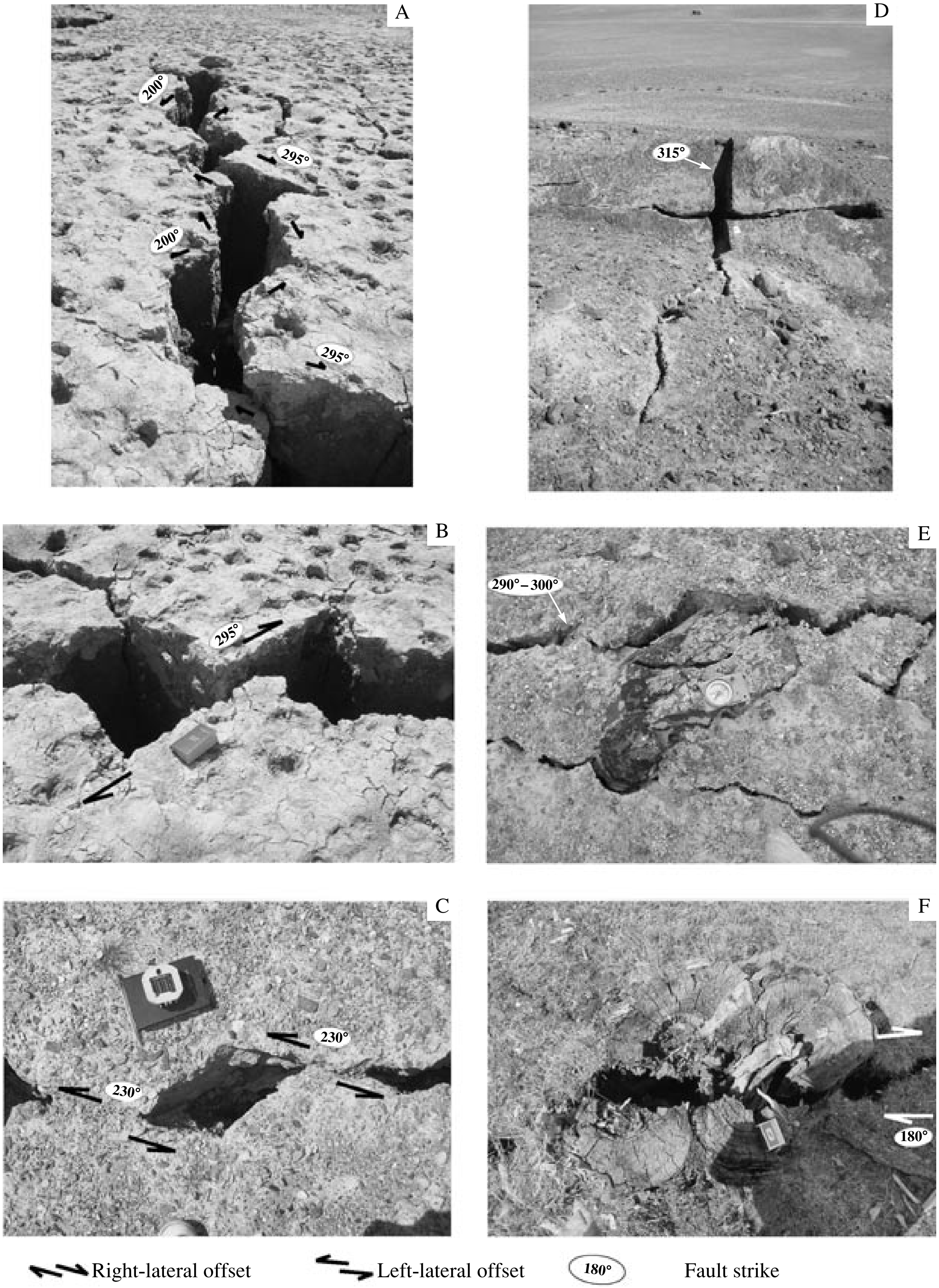

Fig. 5. Close-ups of seismotectonic faults in loose sediments. (A) Fault that consists of separate small fractures, (B) rhomb-shaped blocks, (C) structural features of the pull-apart type, (D) seismotectonic fault in loose sediments that splits a boulder more than 3 m in size, (E) fractures that cut pebbles and soil in the same direction, and (F) right-lateral offset of a stump along the near-meridional fault close to the intersection of several seismotectonic faults; an offset is untypical of the general structural situation.

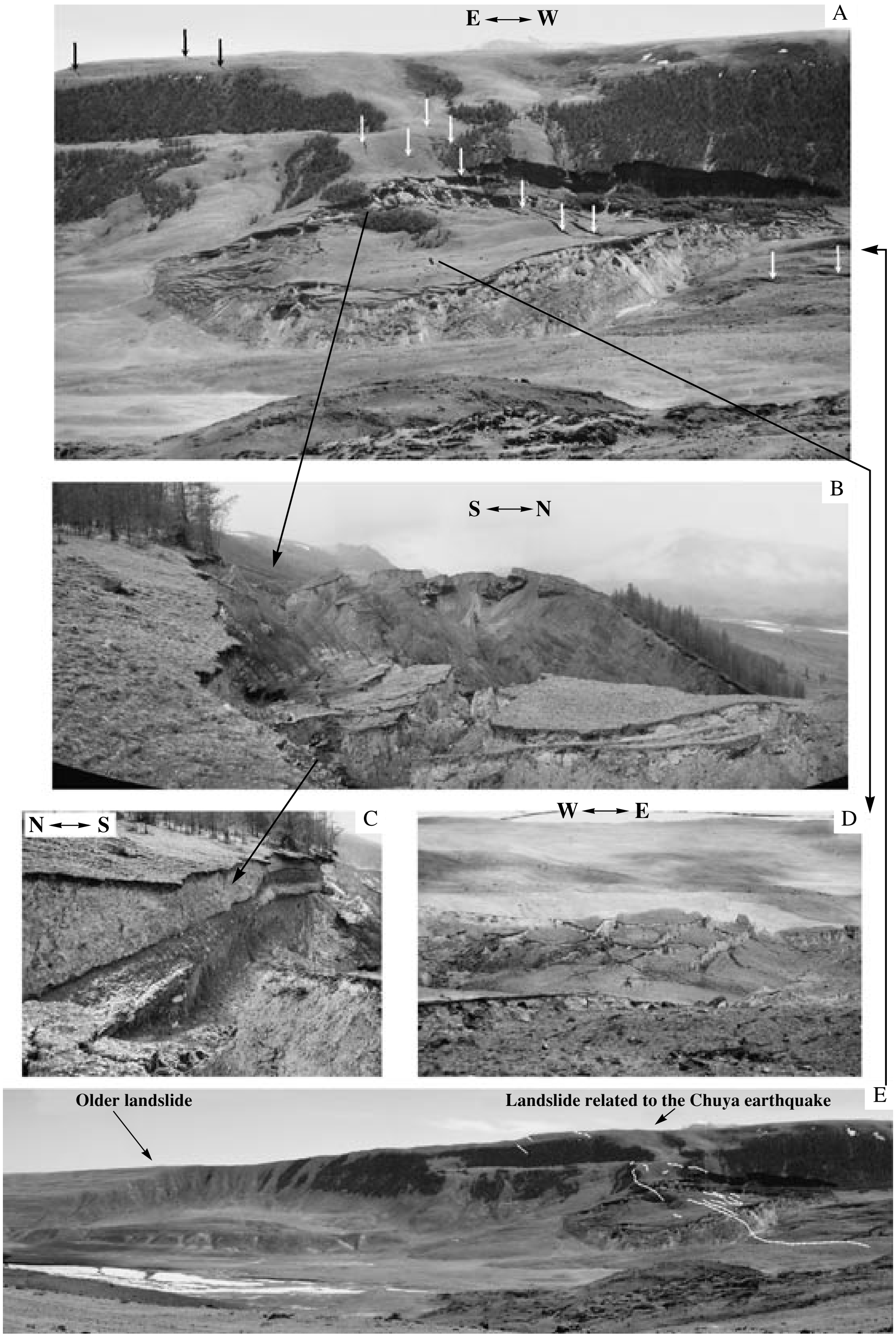

Fig. 6. Seismic landslide formed during the Chuya earthquake in the Taltura River valley. (A) General view, (B) back portion of seismic landslide, (C) tear-off wall in back portion, (D) fracture systems that break landslide into blocks, and (E) older and newly formed landslides. The main faults are indicated in the photographs with dashed lines and arrows.

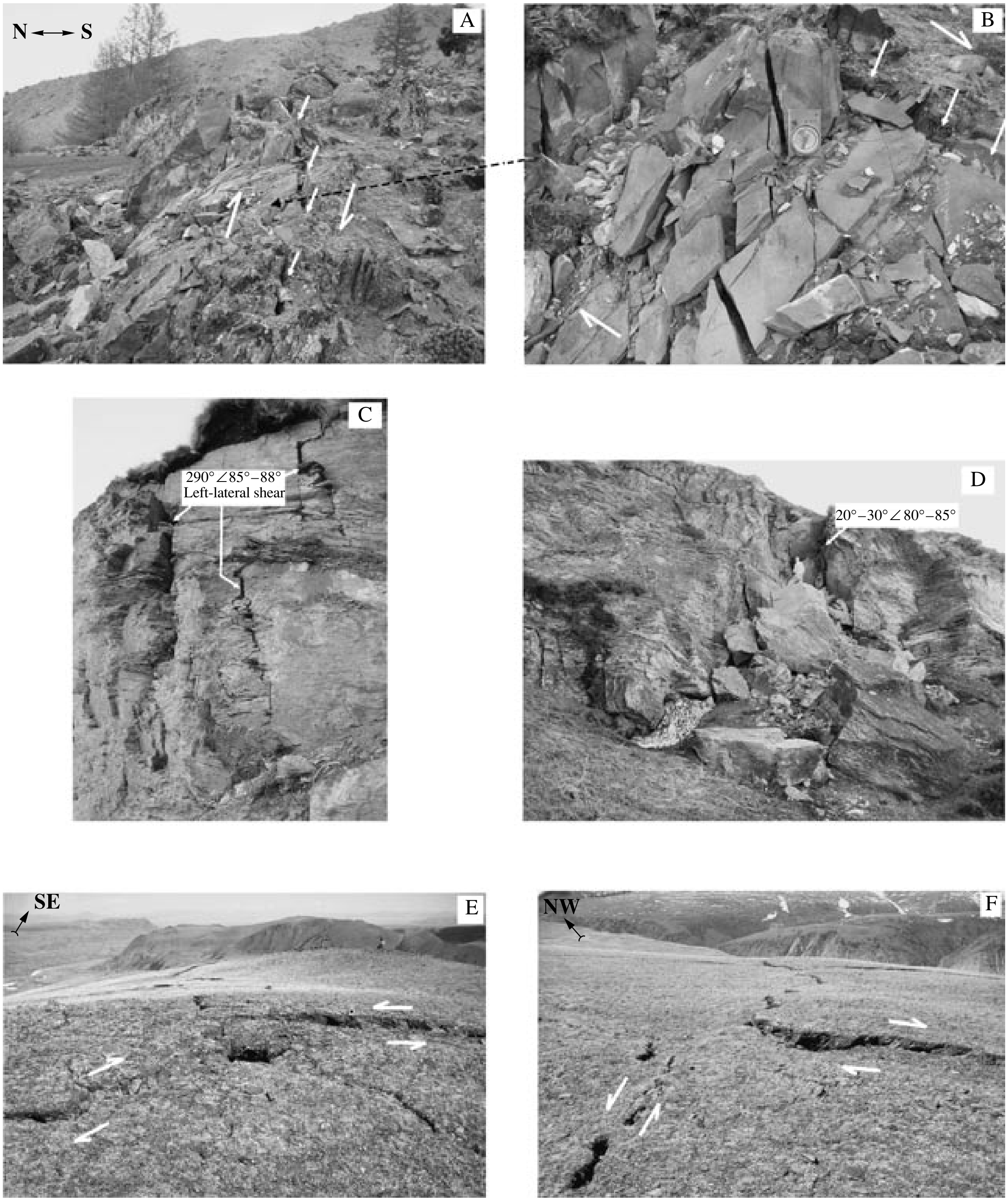

Fig. 7. Seismotectonic deformations (denoted by arrows) in bedrocks related to the Chuya earthquake. (A) Reactivation (opening) of an older shear zone (dip azimuth is 30° (210°); dip angle is 85°–88°) at OP 0205, (B) newly formed and rejuvenated fractures that are en echelon arranged relative to the main right-lateral fault plane (close-up of panel A), (C) signs of fast propagation of the previously existing steeply dipping fractures at OP 0504, (D) zone of rough crushing that was formed during the earthquake at OP 0504, and (E, F) intersections of seismotectonic faults that formed during the Chuya earthquake at the top of Mount Nomodokl at OP 0503.

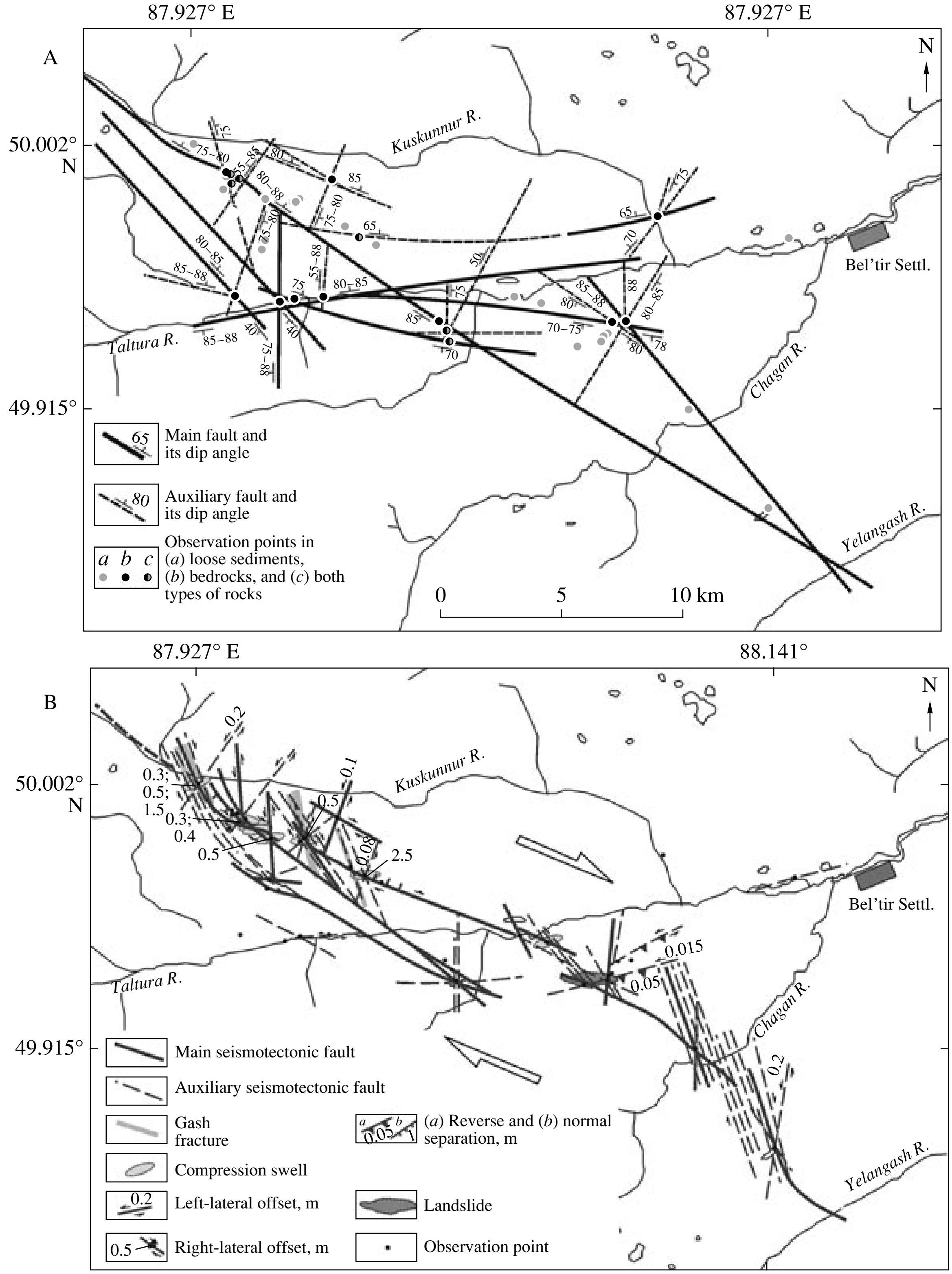

Fig. 8. Fault pattern of the studied area. (A) Network of faults that existed before the Chuya earthquake and (B) internal structure of the fault zone formed during the Chuya earthquake.

strike-slip faults; and the near-latitudinal reverse faults, occasionally with an insignificant strike-slip component.

A comparison of the previously existing and newly formed fault and fracture networks (Fig. 8) shows that the system of seismic dislocations of the Chuya earthquake inherits the older structure to a certain extent. The long, NW- and WNW-trending faults cut open the older shear zones (Fig. 7A). The shorter and en echelon arranged fracture systems are often oriented at an angle to the latter. We suggest that the NW-trending faults mapped in the older rocks are fragments of the large pre-Cenozoic fault zone. Its particular segments probably are currently active as depicted in Fig. 1A, where a series of the NW-trending faults is shown to bound the southwestern wall of the Kurai–Chuya system of basins. The near-latitudinal fault along the Taltura River was reactivated during the Chuya earthquake much more weakly. While forming a system that extends as a southward convex arc, the seismotectonic faults of this direction were reactivated and formed anew farther south.

Analysis of Diagrams of Fracturing and Stress Fields

Diagrams of mass measurements of fracture orientation show that the systems that correspond to R- and R'-shears in the NW-trending right-lateral strike-slip fault zone are most pronounced in loose sediments (Fig. 9A) except for some particular cases. As a rule, the NW-, NNW-, NE-, and NNE-trending maximums of fracturing correspond to R- and R'-shears. These shears are also clearly expressed in bedrocks that are cut by the older NW-trending faults or that remain only weakly broken (Fig. 9B, OPs 0203, 0205, 0206, 0302, 0501, 0503, 0504). The structural patterns displayed in diagrams are often similar to the fracturing patterns in loose sediments (Fig. 9B, OPs 0205, 0302, 0501, 0504). In the near-latitudinal fault zones, R-shears (Fig. 9B, OPs 0402, 0102), R'-shears (Fig. 9B, OPs 0502, 0204), or both (Fig. 9B, OP 0301) are often obscured. In general, as judged from the diagrams of mass measurements (Figs. 9A, 9B) and the synoptic diagrams of fracturing maximums (Fig. 9C), most R-shears and the master seismotectonic fault dip at an angle of 80° to the NNE.

During analysis of the diagrams of fracturing with the Nikolaev method [11], one pair or, less frequently, two pairs of conjugated fracture systems may be distinguished (Figs. 9A, 9B); no conjugated fractures were observed at OP 0502 (Fig. 9B). The reconstruction of stress fields shows that the solutions obtained for loose sediments and bedrocks are very similar (Figs. 9A, 9B). Most of these stress fields correspond to the strike-slip type. Compressive vector σ_1 and tensile vector σ_3 have an inclination of 0°–30°, while the intermediate vector σ_2 has an inclination of 61°–90°. Compressive vector σ_1 declines largely in the NNW–SSE and N–S directions, while tensile vector σ_3 declines in the near-latitudinal direction. At OPs 0103, 0401 (Fig. 9A), and 0205 (Fig. 9B), the axes of tension and compression change places; i.e., σ_1 declines in the near-latitudinal direction, while σ_3 declines in the near-longitudinal direction. Such variations of the stress state have been pointed out previously in studies of fault zones of different morphogenetic types and accounted for by a short-term change of relative values of stresses along with retention of their spatial orientation during fracturing within a rock massif [14, 21]. In our study, two solutions with opposite arrangement of σ_1 and σ_3 at OP 0401, 0205 have been obtained from the analysis of seismotectonic fractures that were formed anew and rejuvenated during one sequence of seismic events. Thus, reorientation of the principal stress axes may occur virtually instantaneously.

The type of stress field changes in some cases from one massif to another or within the same massif only owing to the increase in inclination of compressive axis relative to the horizon. Hence, the solutions that fit tension combined with shear ((σ_1) 31°–60°, (σ_2) 31°–60°, (σ_3) 0°–30°) were obtained at OPs 0503, 0302, and 0204 (Fig. 9B); the solution that corresponds to pure tension ((σ_1) 61°–90°, (σ_2) 0°–30°, (σ_3) 0°–30°) was obtained at OP 0301 (Fig. 9B). At the same time, the shear stress field with a similar near-latitudinal orientation of the tension axis has been restored with the kinematic method [32] (Fig. 9D). If it is kept in mind that OP 0301 is located in the steeply dipping fault zone traced along the Taltura River, it may be suggested that the variations of stress field are caused by an effect of the aforementioned structural feature.

Note that the changes in the type of stress field are also observed in mechanisms of the sources of aftershocks related to the 2003 Chuya earthquake. Reverse and normal mechanisms are noted for most shears (Fig. 1A). According to the seismologic and structural geologic data, the compression axes often change their direction from the meridional to the north-northwestern or the north-northeastern directions.

In general, the internal structure of the fault zone (orientation of R- and R'-shears, compressive and extension structural features, see Figs. 4A, 4D–4F), the measured offsets (Figs. 4B, 4C), diagrams of fracturing (Figs. 9A–9C), and slickenside striation (Fig. 9D) testify to the initial shear stress field that eventually led to the formation of the entire assemblage of seismotectonic deformations related to the Chuya earthquake. This field is characterized by the NNW, almost longitudinal direction of σ_1 and the ENE, almost latitudinal direction of σ_3. This solution is consistent with the mechanism of the main shock of the seismic events on September 27, 2003 (Fig. 1A; the Harvard catalog of earthquakes, http://www.seismology.harvard.edu).

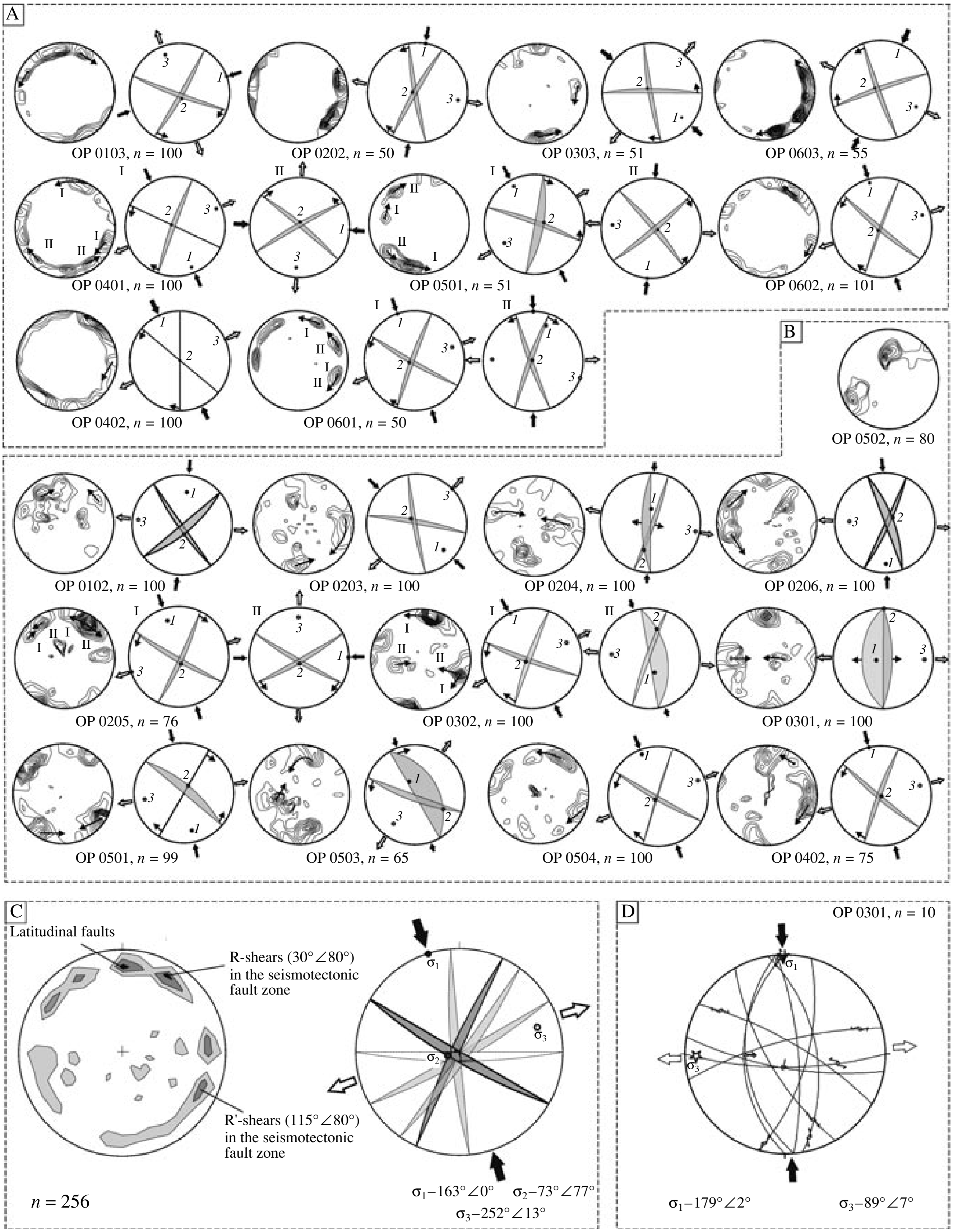
A
OP 0103, n = 100
OP 0202, n = 50
OP 0303, n = 51
OP 0603, n = 55
OP 0401, n = 100
OP 0501, n = 51
OP 0602, n = 101
OP 0402, n = 100
OP 0601, n = 50
B
OP 0502, n = 80
OP 0102, n = 100
OP 0203, n = 100
OP 0204, n = 100
OP 0206, n = 100
OP 0205, n = 76
OP 0302, n = 100
OP 0301, n = 100
OP 0501, n = 99
OP 0503, n = 65
OP 0504, n = 100
OP 0402, n = 75
C
Latitudinal faults
R-shears (30°∠80°) in the seismotectonic fault zone
R'-shears (115°∠80°) in the seismotectonic fault zone
n = 256
σ_1
σ_2
σ_3
σ_1–163°∠0°
σ_2–73°∠77°
σ_3–252°∠13°
D
OP 0301, n = 10
σ_1
σ_3
σ_1–179°∠2°
σ_3–89°∠7°

DISCUSSION

In tectonophysics, the term *fault zone* is treated in a broad sense because such zones include not only the fault plane proper but also much greater bodies of rocks that experience ductile deformation and brittle failure genetically related to the faulting [14]. This definition is based on the well-known works on faults and fault zones, including shears and shear zones [16, 18, 27, 29, 31]. In terms of such an approach, the fault zone as a volumetric deformational element is characterized by an internal structure, i.e., by a set of structural features (elements) that determine the structure of the fault zone and distinguish it from the adjacent space [14]. This set of structural elements is described by the well-known Riedel model. Our results indicate that the system of seismotectonic fractures and other accompanying deformations related to the Chuya earthquake is exactly such a zone that extends in the NW direction. The set of deformations within this fault zone is a structural assemblage that formed in the dynamic setting corresponding to the right-lateral strike-slip fault. The width of the fault zone reaches 4 km, as determined by the location of the outermost observation points that have recorded the NW-trending seismotectonic fractures (Fig. 8B).

As has been shown by experiments, the development of fault zones that are localized in the homogeneous rock massif, loaded similarly along their strike, and deformed at a constant rate nonetheless remains inhomogeneous [14, 16]. This conclusion is also applicable to natural, long-lived faults [14, 23, 26]. The main object of this study is a shear zone that was formed virtually instantaneously either over tens of seconds to a few minutes if the main shock on September 27, 2003, is considered or over 5 days if both the main shock with $M_s = 7.5$ and the strongest aftershock with $M_s = 7.0$ that happened on October 1, 2003, are considered (M_s is given after the Harvard catalog of earthquakes). Nevertheless, the faulting in this case is nonuniform, primarily as concerns the spatial distribution of fractures that is reinforced by structural and compositional heterogeneity of the Earth's crust. Further, the nonuniformity is manifested in rearrangements of the regional stress field in local segments of the fault zone, where σ_1 and σ_3 change places or σ_1 deviates from horizontal position in front of the newly formed or already existing fault. Such a local change of the initial dynamic setting occurred largely near steeply dipping latitudinal faults that hampered the relaxation of the accumulated compressive stress acting in the meridional direction. As a result, small strike-slip displacements (cuttings) and occasional small gaps arose along these faults. The new near-latitudinal seismotectonic faults of reverse character were formed apart from the older faults of the same directions.

According to the physical and structural criteria, the development of the fault zone may be subdivided into three main stages [14]: (1) the early stage of faulting (appearance of the first R-shears); (2) the late stage of faulting, when R-shears are merged into larger faults accompanied by small normal and reverse faults; and (3) the final stage of ultimate failure with formation of the common main fault (Fig. 10). These stages are separated from one another by moments of structural rearrangement and appearance of the main fault plane. Because the detailed study of the Yelangash–Kuskunnur segment has shown that the system of seismotectonic deformations is a fault zone with all its typical attributes, we compared the map of faults and fractures (Fig. 8B) with a theoretical scheme of the formation of internal structure within a strike-slip fault zone with a right-lateral offset (Fig. 10). The comparison has shown that the fault zone of the Chuya earthquake corresponds to the late stage of the evolution when the main fault is still not formed completely but its particular segments are already outlined quite distinctly. According to the curve $\sigma = f(\varepsilon)$ shown in Fig. 10, the loaded body of the Earth's crust, where a system of seismic dislocations has arisen, passed the elastic state with completely reversible deformation (segment OA), strengthening (segment AB), and the state of slackening (segment BC). Point B corresponds to the moment of the main structural rearrangement after the appearance of the first fractures. Thus, it may be said with confidence that the faulting in different rock types follows the general laws of deformation of solids even at the surface and at a high rate of deformation. The seismic event on September 27, 2003, is a spectacular example of a fault-forming earthquake that displays the current geodynamic regime of the Gorny Altai. The study of the system of seismotectonic deformations at the surface and in the upper crust and the comparison of this system with a

Fig. 9. Diagrams of mass measurements of fractures and restored orientation of principal normal stresses. Projection on the upper hemisphere. The window dimension is 10°. σ_1 is the compression axis, σ_2 is the intermediate axis, and σ_3 is the tension axis. (A) Diagrams of mass measurements of fractures in loose sediments and the respective stress-field solution at observation points. Contour lines of the density of fracturing maximums are spaced at 3.5, 4.5, 5.5, 6.5% and more. Arrows inside the diagrams denote preferential directions of scattering in maximums of fracturing that indicate conjugation fracture systems, after the Nikolaev method [11]. The pairs of conjugated fracture systems are denoted by Roman numerals. The observation point numbers and numbers of measurements (n) are placed under each diagram. (B) Diagrams of mass measurements of fractures in bedrocks and the respective stress-field solution at observation points. Contour lines of density of fracturing maximums are spaced at 1.5, 2.5, 3.5, 4.5% and more. See panel A for further explanation. (C) Synoptic diagram of maximums of fracturing constructed from the data presented in panels A and B and the stress-field solution deduced from conjugated systems of R- and R'-shears. Contour lines of the density of fracturing maximums are spaced at 1.5, 2.5, and 3.5%. (D) Stress-field solution for OP 0301 deduced from fault-slip striation, after the Yamaji technique [32].

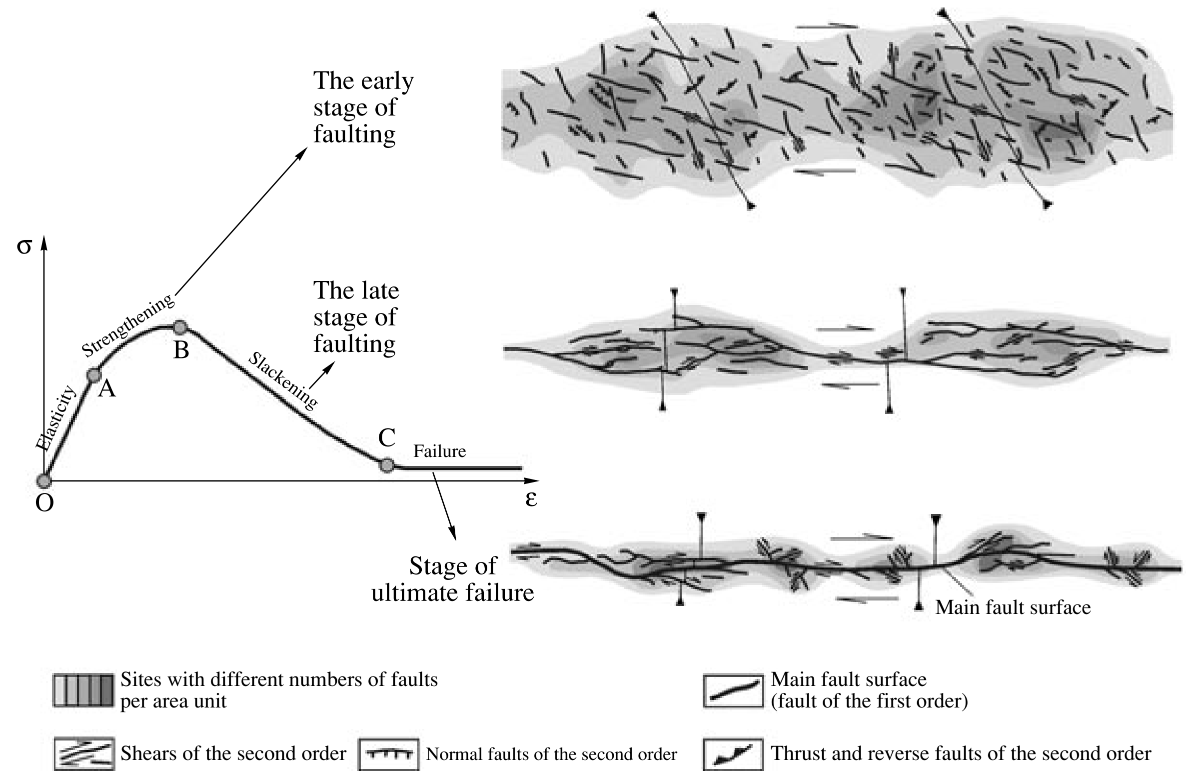

Fig. 10. Formation of the internal structure of a right-lateral fault zone: a conceptual scheme, after [14]. The main stages of faulting correspond to three characteristic segments of the loading (σ)–deformation (ε) curve.

tectonophysical model of faulting in large continental fault zones with a right-lateral offset of walls lead to the conclusion that this model is applicable to the analysis of deformation that arises virtually instantaneously during a strong earthquake.

CONCLUSIONS

The performed investigation allowed us to characterize in detail the system of seismotectonic deformations related to the 2003 Chuya earthquake for a distance of 30 km and to draw the following conclusions.

(1) The seismotectonic deformations related to the earthquake have been recorded both in the loose sediments as an advanced system of R- and R'-shears, gash fractures, and compressive structural features and in the bedrock massifs, where the older shear zones were reactivated and rejuvenated, the older fractures propagated farther, and new faults and crush zones were formed.

(2) The combination of all types of the newly formed structural features is a common assemblage that consists of (i) the NW- and NNW-trending right-lateral strike-slip faults with normal and pull-apart components of faulting often caused by gravity; (ii) the NE- and NNE-trending left-lateral strike-slip faults; and (iii) near-latitudinal reverse faults, occasionally with an insignificant strike-slip component. The same displacements occurred along the previously existing faults except for steeply dipping near-latitudinal faults that experienced local variations of the stress state that resulted in small strike-slip offsets (cuttings).

(3) The system of seismic dislocations that arose during the earthquake is a NW-trending fault zone no less than 4 km wide with an internal structure that comprises a set of systematically arranged structural elements (R- and R'-shears, gash fractures, and compressive features) typical of the right-lateral strike-slip fault. In terms of tectonophysics, the distribution of advanced fractures corresponds to the late stage of faulting, where the main fault is still not formed completely but its particular segments are already quite distinct.

(4) The initial stress field that provided the formation of the whole assemblage of seismotectonic deformations during the Chuya earthquake fits the shear type with the NNW, almost meridional direction of the compression axis and the ENE, almost latitudinal direction of the tension axis. Local variations of the stress state in rock massifs were expressed in an insignificant shift of σ_1 to the northwest or northeast, in the short-term variations of relative stress values with retention of their spatial orientation as indicated by reorientation of the compression and tension axes, and in an increasing inclination angle of σ_1 in front of the already existing fault.

(5) The comparison of the internal structure of the fault zone that arose during the 2003 seismic event with a tectonophysical model of faulting in large continental strike-slip fault zones with a right-lateral offset of walls has led to the conclusion that this model is applicable to the analysis of deformations that arise virtually instantaneously during a strong earthquake. Hence, the faulting in different rock types follows the general laws of deformation of solids even at the surface and at a high rate of deformation.

ACKNOWLEDGMENTS

This study was partly supported by the Russian Foundation for Basic Research (project no. 04-05-64148), the Foundation for Support of Russian Science, and the Council for Grants of the President of the Russian Federation (grant nos. MK-2596.2004.5 and MK-1645.2005.5).

REFERENCES

1. M. M. Buslov, "Cenozoic and Recent Tectonics, Geodynamics, and Seismicity of Central Asia: Control by Basement Structure and Plumes," in *Recent Geodynamics and Hazardous Natural Processes in Central Asia*, Ed. by K. G. Levi and V. A. San'kov (Inst. Earth Crust, Siberian Div., Russian Acad. Sci., Irkutsk, 2005), pp. 9–11 [in Russian].
2. E. M. Vysotsky, I. S. Novikov, A. R. Agatova, and A. S. Gibsher, "The Pleistoseist Zone and Tectonic Position of the Source of the Chuya Earthquake 2003," Dokl. Akad. Nauk **395** (4), 499–502 (2004) [Dokl. Earth Sci. **395A** (3), 328–330 (2004)].
3. E. M. Vysotsky, I. S. Novikov, I. R. Agatova, et al., "Structure of Surface Deformation Zone of the Chuya Earthquake 2003 (Gorny Altai)," in *Relief-Forming Processes: Theory, Practice, and Research Methods* (Inst. Geol., Siberian Div., Russian Acad. Sci., Novosibirsk, 2004), pp. 65–67 [in Russian].
4. A. R. Geodakov, A. N. Ovsyuchenko, S. G. Platonova, and E. A. Rogozhin, "Preliminary Data on the Strong Earthquake 2003 in the Gorny Altai," Vestn. Otd. Nauk Zemli, No. 1 (21) (2003). URL: http:// www.scgis.ru/russian/cp1251/h dgggms/1-2003/screp-8.pdf.
5. M. V. Gzovsky, *Principles of Tectonophysics* (Nedra, Moscow, 1975) [in Russian].
6. S. V. Gol'din, V. S. Seleznev, A. F. Emanov, et al., "The Chuya Earthquake and Its Aftershocks," Dokl. Akad. Nauk **395** (4), 534–536 (2004) [Dokl. Earth Sci. **395A** (3), 394–396 (2004)].
7. E. V. Devyatkin, *Cenozoic Sediments and Neotectonics of the Southeastern Altai* (Nauka, Moscow, 1965) [in Russian].
8. N. D. Zhalkovsky, O. A. Kuchai, and V. I. Muchnaya, "Seismicity and Some Characteristics of the Stress State of the Earth's Crust in the Altai–Sayan Region," Geol. Geofiz. **36** (10), 20–30 (1995).
9. O. A. Kuchai, "Seismotectonic Deformations of the Earth's Crust in the Altai–Sayan Region from Data on Earthquake Source Mechanisms and Aftershocks," in *Methods of Analysis of Geodynamic Setting Prediction of Seismic Events* (KNIIGiMS, Krasnoyarsk, 2005), pp. 17–20 [in Russian].
10. O. V. Lunina, A. S. Gladkov, I. S. Novikov, and A. R. Agatova, "Tectonophysical Analysis of Fault Deformation Zone of the Chuya Earthquake, September 27, 2003," Dokl. Akad. Nauk **401** (1), 58–61 (2005) [Dokl. Earth Sci. **401** (2), 197–199 (2005)].
11. P. N. Nikolaev, *Technique of Tectonodynamic Analysis*, Ed. by N. I. Nikolaev (Nedra, Moscow, 1992) [in Russian].
12. I. S. Novikov, *Morphotectonics of Altai* (Izd. Sib. Otd. Ross. Akad. Nauk, Filial GEO, Novosibirsk, 2004) [in Russian].
13. E. A. Rogozhin and S. G. Platonova, *Holocene Earthquake Source Zones of Holocene Strong Earthquakes in the Gorny Altai* (Joint Inst. Physics of the Earth, Russian Academy of Sciences, Moscow, 2002) [in Russian].
14. K. Zh. Seminsky, *Inner Structure of Continental Fault Zones. Tectonophysical Aspect* (Izd. Sib. Otd. Ross. Akad. Nauk, Filial GEO, Novosibirsk, 2003) [in Russian].
15. V. Yu. Timofeev, D. G. Ardyukov, E. A. Zapreeva, et al., "Fields and Models of Displacements in the Chuya Earthquake Zone in the Southern Gorny Altai," in *Recent Geodynamics and Hazardous Natural Processes in Central Asia*, Ed. by K. G. Levi. and V. A. San'kov (Inst. Earth Crust, Siberian Division, Russian Acad. Sci., Irkutsk, 2005), pp. 293–295 [in Russian].
16. S. I. Sherman, K. Zh. Seminsky, S. A. Bornyakov, et al., *Faulting in the Lithosphere. Shear Zones* (Nauka, Novosibirsk, 1991) [in Russian].
17. S. L. Yunga, "Seismotectonic Deformations of the Northern Eurasian Fold Belts in the Neotectonic Phase," Fiz. Zemli **32** (12), 37–58 (1996) [Izv. Physics Solid Earth **32** (12), 955–974 (1996)].
18. N. N. Ambraseys, "Some Characteristic Features of the Anatolian Fault Zone," Tectonophysics **9**, 143–165 (1970).
19. J. Angelier, "Tectonic Analysis of Fault Slip Data Sets," J. Geophys. Res. **89**, 5835–5848 (1984).
20. I. Baljinnyam, A. Bayasgalan, B. A. Borisov, et al., *Ruptures of Major Earthquakes and Active Deformation in Mongolia and Its Surrounding* (Geol. Soc. Am. Mem., 1993), Vol. 181.
21. R. Caputo, "Stress Variability and Brittle Tectonic Structures," Earth-Science Rev. **70**, 103–127 (2005).
22. N. L. Dobretsov, M. M. Buslov, D. Delvaux, et al., "Meso- and Cenozoic Tectonics of the Central Asian Mountain Belt: Effect of Lithospheric Plate Interaction and Mantle Plume," Intern. Geol. Rev. **38**, 430–466 (1996).
23. Y.-S. Kim, D. C. P. Peacock, and D. J. Sanderson, "Fault Damage Zones," J. Struct. Geol. **26**, 503–517 (2004).
24. A. N. Leontyev and E. A. Rogozhin, "Long-Term Geological Factors of Seismicity (Exemplified by the Sayan-Altai Fold Area)," J. Earthquake Prediction Res. **4** (3), 320–339 (1995).

25. P. Molnar and P. Tapponier, “Cenozoic Tectonics of Asia: Effect of Continental Collision,” Science **189**, 419–426 (1975).

26. M. A. Pachell and J. P. Evans, “Growth, Linkage, and Termination Processes of a 10-km-Long Strike-Slip Fault in Jointed Granite: the Gemini Fault Zone, Sierra Nevada, California,” J. Struct. Geol. **24**, 1903–1924 (2002).

27. J. G. Ramsay, “Shear Zone Geometry: A Review,” J. Struct. Geol. **2**, 83–89 (1980).

28. E. A. Rogozhin, B. M. Bogachkin, Yu. V. Nechaev, et al., “Paleoseismological Investigations on the Territory of Russian (Gorny) Altai,” J. Earthquake Prediction Res. **7** (4), 391–413 (1998).

29. A. M. S. Şengör, N. Gorur, and F. Saroglu, “Strike-Slip Faulting and Related Basin Formation in Zones of Tectonic Escape: Turkey as a Case Study,” Soc. Econ. Geol. Paleontol. Mineral. Spec. Publ. **37**, 227–264 (1985).

30. A. M. S. Şengör, B. Natal’in, and V. S. Burtman, “Evolution of the Altaid Tectonic Collage and Palaeozoic Crustal Growth in Eurasia,” Nature **364** (6435), 299–307 (1993).

31. A. G. Sylvester, “Strike-Slip Faults,” Geol. Soc. Am. Bull. **100**, 1666–1703 (1988).

32. A. Yamaji, “The Multiple Inverse Method: A New Technique to Separate Stresses from Heterogeneous Fault-Slip Data,” J. Struct. Geol. **22**, 441–452 (2000).

Reviewers: E.A. Rogozhin and N.V. Koronovskii